Science of the Total Environment 818 (2022) 151800

Contents lists available at ScienceDirect

Science of the Total Environment

journal homepage: www.elsevier.com/locate/scitotenv

Source identification and characterization of organic nitrogen in atmospheric aerosols at a suburban site in China

Lu Qi [a,b], Carlo Bozzetti [a,1], Joel C. Corbin [a,2], Kaspar R. Daellenbach [a], Imad El Haddad [a], Qi Zhang [c], Junfeng Wang [b], Urs Baltensperger [a], André S.H. Prévôt [a,*], Mindong Chen [b], Xinlei Ge [b,*], Jay G. Slowik [a,*]

[a] Laboratory of Atmospheric Chemistry, Paul Scherrer Institute (PSI), 5232 Villigen, Switzerland
[b] Jiangsu Key Laboratory of Atmospheric Environment Monitoring and Pollution Control, Collaborative Innovation Center of Atmospheric Environment and Equipment Technology, School of Environmental Science and Engineering, Nanjing University of Information Science & Technology, Nanjing 210044, China
[c] Department of Environmental Toxicology, University of California, Davis, CA 95616, USA

HIGHLIGHTS

- Characterization of organic nitrogen (ON) ions
- Quantify the sources of ON in submicron aerosols
- Comparison between regular organic aerosol PMF analysis and PMF_ON analysis.

GRAPHICAL ABSTRACT

The retrieved PMF ON factors were defined as: Oxygenated secondary OA (OOA_{ON}), amine-related OA ($AMOA_{ON}$), hydrocarbon-like OA (HOA_{ON}), industry OA (IOA_{ON}), and local primary OA (POA_{ON}).

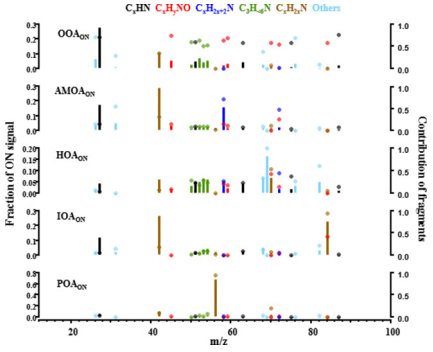

ARTICLE INFO

Article history:
Received 9 September 2021
Received in revised form 14 November 2021
Accepted 15 November 2021
Available online 20 November 2021

Editor: Pingqing Fu

Keywords:
Organic nitrogen
Source apportionment
PMF_ON

ABSTRACT

Despite the fact that atmospheric particulate organic nitrogen (ON) can significantly affect human health, ecosystems and the earth's climate system, qualitative and quantitative chemical characterization of ON remains limited due to its chemical complexity. In this study, the Aerodyne soot particle - high-resolution time-of-flight aerosol mass spectrometer (SP-AMS) was deployed for ambient measurements in Nanjing, China. Positive matrix factorization (PMF) was applied to the ON data to quantify the sources of ON in submicron aerosols. The averaged ON concentration was 1.24 μg m^{-3}, while the averaged total nitrogen (TN) in the aerosol was 20.26 μg m^{-3}. From the PMF ON analysis, a 5-factor solution was selected as the most representative and interpretable solution for the investigated dataset, including oxygenated OA (OOA_{ON}), amine-related OA_{ON} ($AMOA_{ON}$), hydrocarbon-like OA (HOA_{ON}), industry OA (IOA_{ON}), and local primary OA (POA_{ON}) factors. The quantified ON ions were separated into families, including C_xHN, C_xH_yNO, $C_3H_{<6}N$, $C_xH_{2x+2}N$, $C_xH_{2x}N$ and Others, consistent with their contribution to each factor. The C_xH_yNO family mainly contributed to the OOA_{ON} factor and suggested the presence of amides or amino acids. The $C_xH_{2x+2}N$ family likely mostly originated from amines only contributing to the $AMOA_{ON}$ and HOA_{ON} factors. The IOA_{ON} and POA_{ON} factors were resolved due to significant tracers in the mass spectra. Further, compared with regular organic PMF analysis, PMF ON analysis gave more insights due to improved source separation and interpretability of the OA components, which could be a role model for further atmospheric ON research.

* Corresponding authors.
E-mail addresses: andre.prevot@psi.ch (A.S.H. Prévôt), caxinra@163.com (X. Ge), jay.slowik@psi.ch (J.G. Slowik).
[1] Datalystica Ltd., Park innovAARE, 5234 Villigen, Switzerland.
[2] Metrology Research Centre, 1200 Montreal Road, Ottawa K1A 0R6, Ontario, Canada.

http://dx.doi.org/10.1016/j.scitotenv.2021.151800

1. Introduction

Atmospheric organic nitrogen (ON) has been ubiquitously observed in atmospheric aerosol particles and aqueous droplets (e.g., fog/cloud water, and rainwater). This fraction may represent ~30% of total (gaseous and particulate) airborne nitrogen (Cape et al., 2011). In the following, ON always refers to particulate ON unless specified otherwise. Atmospheric ON is less understood than inorganic nitrogen (IN: ammonium, nitrate and nitrite), since it consists of a wide array of compounds, which in turn have a great variety of molecular weight, functionality, and physicochemical properties (Saxena and Hildemann, 1996). Furthermore, ON emissions may result from a diverse array of sources and may undergo much more complex atmospheric transformations than IN. These transformations govern the spatial and temporal variation of ON in the atmosphere. ON plays an important role in the nitrogen cycle of terrestrial and aquatic ecosystems owing to its bioavailability (Neff et al., 2002; Seitzinger and Sanders, 1999; Weathers et al., 2000; Cornell et al., 1995; Cornell, 2011). ON species can also influence the optical (Nguyen et al., 2012; Zarzana et al., 2012; Powelson et al., 2013; Lee et al., 2013; Chen et al., 2018; Chen et al., 2020; Mohr et al., 2013) and hygroscopic properties (Chan et al., 2005; Qiu and Zhang, 2012; Clegg et al., 2013; Hu et al., 2014; Sauerwein et al., 2015) of aerosol particles and fog/cloud droplets.

Bulk quantification of total ON (nitrogen mass contained in N-containing organics) is typically determined as the mass difference between total nitrogen (TN) and IN, i.e., ON = TN – IN (e.g., Ho et al., 2015; Chen et al., 2019). Concentrations of IN components can be measured individually using techniques such as ion chromatography, while measurement of TN involves the conversion of all N-containing species into inorganic forms, e.g., NO_3^-, NO_2^-, and NH_4^+ or nitrogen containing inorganic and organic gases, e.g., NO_x, NH_3, or peroxyacyl nitrates (Cornell et al., 2003) using approaches of photochemical, chemical, and high-temperature oxidations (Jickells et al., 2013). Note that these methods often lead to large uncertainties in ON quantification due to the risk of not oxidizing all ON compounds, and the aggregation of measurement errors, especially when ON is minor in the sample (Cornell et al., 2003;Cape et al., 2011). In addition, traditional filter collection may cause hydrolysis, partitioning, or filter collection artifacts, the measurement of TN or IN is very artifact-prone because of the semi-volatile nature of NH_4NO_3, and the low time resolution, ranging from hours to days, is often insufficient to describe source variation or reactive processes.

Extensive speciation analyses of ON have been conducted. A large number of ON compounds with different functional groups have been identified using analytical techniques including ion chromatography, liquid chromatography - mass spectrometry (LC-MS), and high-resolution electrospray ionization mass spectrometry (ESI-MS) (Ruiz-Jimenez et al., 2012;Samy and Hays, 2013;Samy et al., 2013;Samy et al., 2011;Junninen et al., 2010;Angelino et al., 2001;Huang et al., 2012;Sun et al., 2011b;Smith et al., 2010). The ON species identified include amines, amino acids, urea, amides, nitriles, organic nitrates, nitro-compounds, and N-heterocyclic compounds, etc. However, these identified ON classes, individually, often account for only a small fraction of the total ON, (with e.g., <20% from amino compounds (Zhang and Anastasio, 2003, Zhang and Anastasio, 2001;Zhang et al., 2002)), or they are not quantified, limiting detailed understanding of ON chemistry.

A high-resolution time-of-flight chemical ionization mass spectrometer (HR-ToF-CIMS) using iodide-adduct ionization with a filter inlet for gases and aerosols (FIGAERO) which allows alternating in situ measurements of the speciated ON in gas and particle phases at molecular level was recently developed (Lopez-Hilfiker et al., 2014). However, simple alkyl or keto nitrates are underestimated or not detected at all by this technique. Indeed, quantitative treatment of FIGAERO measurements is complicated by differences in instrument sensitivity to different compounds, which complicates not only the interpretation of the ON composition, but also the total ON/IN relationship. Furthermore, filter collection and thermal desorption cause loss of organic nitrogen.

The Aerodyne high-resolution aerosol mass spectrometer (HR-AMS) has been widely used (DeCarlo et al., 2006). The HR-AMS possesses unique advantages regarding the bulk quantification, speciation and source apportionment of condensed-phase ON species. The instrument's capability of differentiating ions with the same nominal integer mass allows determination of the chemical formulas of ion fragments from organic aerosol (OA) (Aiken et al., 2007;Aiken et al., 2008), which can be used to estimate the total ON content and provide insight into its composition. The HR-AMS also provides new perspectives for source identification of ON. The highly time-resolved HR-AMS data (typically in minutes) provides rich information to examine the co-variation of ON species with other components with known sources and allows the application of advanced multivariate factor analysis to segregate components with common patterns of their behaviour, thus to infer the particular source types and/or chemical processes. Moreover, as a real-time instrument, AMS avoids the sampling artifacts during sample storage and handling that may affect off-line analyses. Previous studies showed that the spectral patterns of different ON families can provide new insights into sources and processes of ON (Aiken et al., 2009;Sun et al., 2011a;Xu et al., 2017;Struckmeier et al., 2016). However, available AMS research of ON is based on the characterization and source apportionment analysis of organic compounds, which highly limits the understanding of atmospheric ON chemistry. In this study, positive matrix factorization (PMF) was applied to the ON fragments to quantify the sources of ON in submicron aerosols, compared to regular organic PMF analysis, and to assess the ON role in aerosol particles.

2. Methodology

2.1. Sampling site and instrumentation

The sampling site was at the campus of the Nanjing University of Information Science and Technology (32°12′20.82″N, 118°42′25.46″E). The measurement period was from February 20 to March 23, 2015. The site was located west/southwest of an industrial zone (mainly petrochemical, chemical, iron and steelmaking plants), close to a residential area and a few arterial roads (Wu et al., 2018;Wang et al., 2016).

The setup and operation of the SP-AMS were described in our previous publications (Wu et al., 2018; Wang et al., 2016). In brief, the SP-AMS is based on the Aerodyne high-resolution time-of-flight aerosol mass spectrometer (HR-ToF-AMS, Canagaratna et al., 2007), in which non-refractory components are vaporized by impaction on a 600 °C tungsten surface, but also includes an intracavity Nd:YAG laser (1064 nm) allowing it to vaporize light-absorbing aerosols, especially refractory black carbon (*r*BC, C_1^+ – C_{31}^+) (Onasch et al., 2012). Regardless of the vaporization scheme, the resulting gas is ionized by 70 eV electron impact (EI) ionization and detected by a time-of-flight mass spectrometer ($m/\Delta m$ = 5000–6000). In the present study, the instrument alternated between standard collection mode (laser off) and SP mode (laser on) every 5 min. The instrument was calibrated for ionization efficiency (IE) for nitrate every week using 250 nm NH_4NO_3 particles following a mass-based method (Jayne et al., 2000) at standard collection mode. The relative ionization efficiency (RIE) of ammonium was also determined based on these measurements, and RIE of sulfate was calibrated using pure ammonium sulfate separately. The RIEs for nitrate, sulfate, chloride, ammonium and organics were 1.05, 1.18, 1.3, 3.0 and 1.4, respectively. The rBC component is detected mainly in the form of C_n^+ ions and the instrument was operated at an m/z range of up to ~2000 to detect the fullerene ions C_{30}^+– C_{160}^+ (Onasch et al., 2015; Corbin et al., 2014). The rBC calibration was obtained using monodisperse rBC particles and a condensation particle counter (CPC) to measure particle number concentrations.

Ambient air was sampled through a 16.7 L min^{-1} cyclone (~5 m above the ground) to achieve a size cut of 2.5 μm. The concentration of O_3 was acquired from the nearest environmental monitoring site. The meteorological parameters, including air temperature (*T*), relative humidity (RH), wind

speed (WS), wind direction (WD), and solar radiation were measured by a meteorological station ~50 m away from the sampling site.

2.2. Basic SP-AMS data analysis

The SP-AMS data were processed and analysed within Igor Pro 6.36 (Wavemetrics) using the standard ToF-AMS analysis toolkit software package, SQUIRREL (version 1.57) and PIKA (1.16, http://cires1.colorado.edu/jimenez-group/ToFAMSResources/ToFSoftware/). The collection efficiency (CE) was estimated using the composition-dependent method of (Middlebrook et al., 2012). The elemental ratios of OA including nitrogen-to-carbon (N/C), organic mass to organic carbon (OM/OC) and oxygen-to-carbon (O/C) ratios were determined with the Improved-Ambient (I-A) method (Canagaratna et al., 2015).

Here, we used the peak-fitting uncertainty model described by Corbin et al. (2015) instead of the PIKA 1.16 error model to address signal-to-noise ratio (SNR) issues (https://acp.copernicus.org/preprints/acp-2020-890/acp-2020-890-SC1.pdf) in PMF. The Corbin et al. model results are in percentage uncertainties in SNR for isolated peaks (due to uncertainty in peak width) and also potentially much larger uncertainties when small peaks overlap with larger ones. The model was successfully applied to determine overlapping peaks, e.g. CHO and CHN, decreased the fitting artifact. In total, 27 fitted ON ions between m/z 26 and 87 were identified which had been separated from its adjacent major peaks (see Fig. S1 for several examples at m/z 42, 53, and 92).

Most of the ON ions are assigned to five families: C_xHN, CHNO, $C_3H_{<6}N$, $C_xH_{2x+2}N$, and $C_xH_{2x}N$ based on their bulk time series and elemental ratios, plus the following additional ions: CN, CH_5N, C_3H_4N, C_4H_6N, C_4H_7N, C_5H_8N, and C_5H_2N.

The ON and TN in submicron organic aerosols can be determined as

$$OC = organics/\left(\frac{OM}{OC}\right) \tag{1}$$

$$ON = OC * \frac{N}{C} * \left(\frac{14}{12}\right) \tag{2}$$

$$TN = ON + N_{NO_3^-} + N_{NH_4^+} \tag{3}$$

OC is the carbon content of the OA mass; OM/OC and N/C are the elemental ratios determined from elemental analysis; $N_{NO_3^-}$ and $N_{NH_4^+}$ are the nitrogen concentrations in inorganic NO_3 and NH_4 measured by the SP-AMS.

2.3. Source apportionment

Source apportionment using positive matrix factorization (PMF) was performed separately on organic aerosol (denoted PMF OA) and organic nitrogen (denoted PMF ON, only 27 ON ions included). PMF was implemented in the multilinear engine (ME-2), using the SoFi interface (Source Finder, version 6.66; (Canonaco et al., 2013)) programmed in Igor Pro 6.36 (Wavemetrics, Inc.) for model configuration and post-analysis. PMF is a bilinear receptor model which describes measurements as a linear combination of static factor profiles (i.e. characteristic mass spectra), corresponding to specific emission sources and/or atmospheric processes, and their time-dependent source contributions as shown in the following equation (Paatero and Tapper, 1994):

$$x_{ij} = \sum_{k=1}^{p} g_{ik} \times f_{kj} + e_{ij} \tag{4}$$

Here, x_{ij}, g_{ik}, f_{kj}, and e_{ij} are matrix elements of the measurement, factor time series, factor profile, and residual matrices, respectively. The subscripts i, k, and j denote matrix indices corresponding to time of measurement, m/z, and factor, respectively. The measured $\mathbf{X}$ is an $m \times n$ matrix, representing m measurements of n m/z. $\mathbf{G}$ and $\mathbf{F}$ are $n \times p$ and $p \times m$ matrices, respectively, where p is the number of factors contained in a given model solution and is selected by the user.

Eq. (4) is solved using a least squares algorithm that iteratively minimize the quantity Q (Eq. 5), defined as the sum of the squares of the scaled residuals:

$$Q = \sum_i \sum_j \left(\frac{e_{ij}}{\sigma_{ij}}\right)^2 \tag{5}$$

Here, e_{ij} represents the residuals (elements of $\mathbf{E}$), with i and j denoting respectively the time and m/z indices, and $\sigma_{ij}$was the corresponding element in the measurement uncertainty matrix.

The selection of the number of factors was based on an analysis of the dependence of total Q or Q/Q_{exp}, scaled residuals, comparison of factor time series and external tracers, examination of factor diurnal patterns and the evaluation of the residual time series as a function of the number of resolved factors (details in Section 3.2 and Supplement, Fig. S2, S3, S4).

Bootstrap analysis (Davison and Hinkley, 1997) was conducted to determine the statistical stability and uncertainties of the PMF ON solution and to evaluate trends in specific ions. Bootstrap analysis generates a set of new input data and error matrices for analysis from random resampling of the original input data. This resampling perturbs the input data by randomly choosing rows (time points) of the original matrix which are present several times, while other rows are removed (Paatero and Tapper, 1994); the overall dimensions of the data matrix is kept constant for each resampling. We performed 1000 bootstrap runs for a 5-factor solution with all factors unconstrained. Fig. S5 summarizes the averaged extracted solution from the bootstrap analysis, showing the means of these solutions for the time series and mass spectra.

3. Results

3.1. Study overview

Fig. 1 shows the time series of meteorological parameters including temperature (T), relative humidity (RH), solar radiation, wind direction (WD) colored by wind speed (WS), the mass concentration of organic nitrogen (ON, Eq. (2)), total nitrogen (TN, Eq. (3)), PM_1 components (organics, ammonium, nitrate, chloride), and the fractional contributions of OA factors from the original PMF OA analysis (Wu et al., 2018; Wang et al., 2016): salient characteristics of these OA source apportionment factors are discussed in Section 3.2.

As shown in Fig. 1, the temperature varied from 0 °C to 21 °C with a mean value of 8.5 °C, which potentially correlated to ON formation, e.g. March 13–20, the total ON concentration increased with the higher temperature. The weather was generally humid during the sampling period with an average RH of ~70%. The average of the wind speed was around 1.4 m s^{-1} mostly from east/northeast directions. The PM_1 concentration varied from 8.4 to 180.5 μg m^{-3}, with a mean of 46.3 μg m^{-3}, and was dominated by inorganic components (68.4%). A high correlation (R = 0.89) was observed between OA and ON (Fig. S1, discussed in Section 3.4). The average ON concentration in the submicron aerosol is 1.24 μg m^{-3}, while the average TN is 20.26 μg m^{-3}. The ON concentrations determined by the SP-AMS in Nanjing are typically similar to other observations in China, e.g. 1.7 μg m^{-3} (1.4% in $PM_{2.5}$) in Changzhou (Ye et al., 2016, SP-AMS), but lower than others, e.g. 3.17 ± 2.02 μg m^{-3} in Beijing (Duan et al., 2009).

We estimated the concentration of particulate organic nitrate (NO_3_org) based on the AMS data following the approaches in Xu et al. (2015b). The method is based on the NO^+/NO_2^+ ratio (NO_x^+ ratio) in the HR-ToF-AMS. Due to the very different NO_x^+ ratios of organic nitrates and inorganic nitrate (i.e., R_{ON} and $R_{NH_4NO_3}$, respectively; (Fry et al., 2009;Bruns et al., 2010)), the NO_2^+ and NO^+ concentrations of organic nitrates (NO_2, ON and NO_{ON}) can be quantified with the HR-ToF-AMS data using

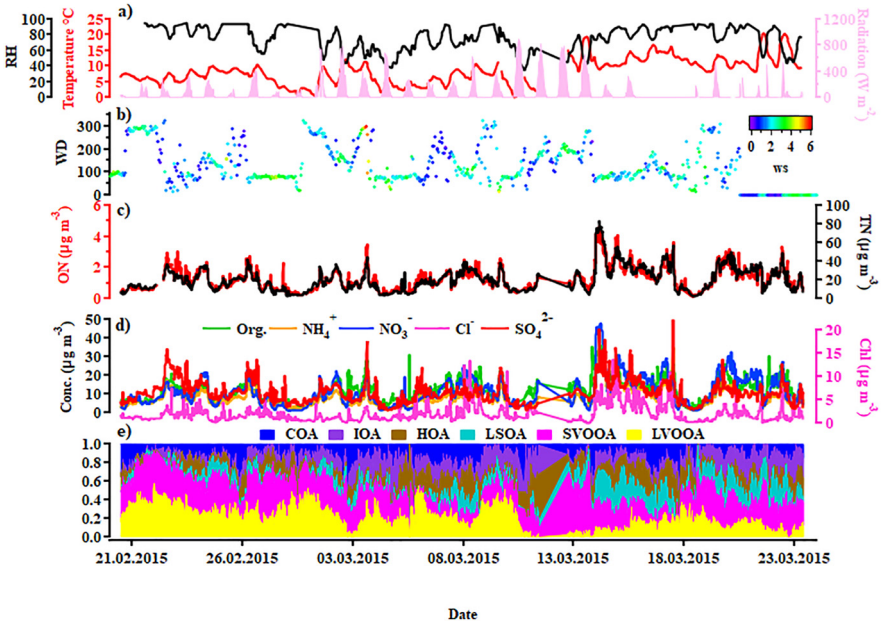

Fig. 1. Overview of the chemical composition and temporal trends of submicron aerosols at Nanjing in February and March 2015 including (a) time series of ambient air relative humidity (*RH*), temperature (*T*), solar radiation; (b) time series of wind direction (WD) colored by wind speed (WS); (c) time series of organic nitrogen (ON) and total nitrogen (TN); (d) time series of the mass concentrations of organic aerosol (Org), nitrate (NO_3^-), sulfate (SO_4^{2-}), ammonium (NH_4^+), chloride (Cl^-) to total PM1; and (e) time series of the mass fractional contributions to total aerosol (OA) of the six factors derived from original PMF analysis (cooking OA (COA), traffic OA (HOA), industry OA (IOA) local secondary OA (LSOA), semi-volatile oxygenated OA (SVOOA), and low-volatility oxygenated OA (LVOOA)).

Eqs. (6) and (7), respectively (Farmer et al., 2010; Kiendler-Scharr et al., 2016; Xu et al., 2015;Yu et al., 2019):

$$NO_{2,ON}^{+} = \frac{NO_{2,obs}^{+} * (R_{obs} - R_{NH_4NO_3})}{R_{ON} - R_{NH_4NO_3}} \quad (6)$$

$$NO_{ON}^{+} = R_{ON} * NO_{2,ON} \quad (7)$$

where R_{obs} is the NO_x^+ ratio from the measurement. R_{NH4NO3} was determined by IE calibration using pure NH_4NO_3 every 2 weeks (Fry et al., 2013). However, the value of R_{ON} is difficult to determine because it varies between instruments and precursor VOCs. In this study, we used R_{ON} as 2.9*R_{NH4NO3} based on literature (Farmer et al., 2010; Kiendler-Scharr et al., 2016; Yu et al., 2019; Xu et al., 2015).

3.2. PMF on organic aerosol (OA)

For the whole dataset, procedures of the PMF analyses, justifications and diagnostics of the optimal PMF OA solution, high resolution mass spectra of the factors and features/behaviors of these factors were presented in Wang et al., 2016 and Wu et al., 2018. Here we briefly summarize the PMF OA source apportionment from these studies and evaluate their ability to explain ON sources.

Six OA factors were identified, i.e., cooking OA (COA), traffic OA (HOA), industry OA (IOA) local secondary OA (LSOA), semi-volatile oxygenated OA (SVOOA), and low-volatility oxygenated OA (LVOOA).

HOA is abundant in hydrocarbon ions, and COA has significant oxygenated ions at $m/z = 55$ and $m/z = 57$; these spectral features and their diurnal patterns are both similar to the ones identified at other locations (Sun et al., 2011a, 2011b). A specific IOA factor was separated: it has a relatively high fraction of CO_2^+, and its temporal variation behaves very differently compared to HOA ($r^2 = 0.03$) and COA ($r^2 = 0.01$) (although the diurnal trend of IOA is somewhat similar to that of HOA). SVOOA and LVOOA also have similar features with those identified by the AMS community: SVOOA has a smaller $CO_2^+/C_2H_3O^+$ ratio than LVOOA; SVOOA correlates better with nitrate ($r^2 = 0.53$) than with sulfate ($r^2 = 0.31$) while LVOOA correlates better with sulfate ($r^2 = 0.46$) than with nitrate ($r^2 = 0.26$). In addition, an LOOA factor was also identified, accounting for a relatively smaller mass fraction (10%) of the total OA than other factors. The average contribution from POA (48%, (COA, 15.5%), (HOA, 20%), (IOA, 16.5%)) was almost equal to that of SOA (52%, local oxygenated OA (LOOA, 10%), semi-volatile oxygenated OA (SVOOA, 16.4%), low-volatility oxygenated OA (LVOOA, 21.6%)).

Fig. 2 shows the ON apportionment in these PMF OA solutions, colored by six families: C_xHN, CHNO, $C_3H_{<6}N$, $C_xH_{2x+2}N$, $C_xH_{2x}N$ and others. The left axis presents the relative composition of each factor and the right axis the relative contribution of each factor to the given ON ions. Accordingly, no specific mass spectral signature and/or striking differences of relative contributions to these ON ions for each factor are identified since almost all families and all ions appeared in every factor. Only minor differences can be observed, e.g. the $C_xH_{2x}N$ family (especially at large mass-to-charge ratios) has high contributions to the POA factors. The lack of discrimination is likely due to much lower concentrations and lower signal to noise of ON ions compared to other OA ions with high concentrations and high signal to noise. It is not possible to represent well the attribution of ON using the original PMF method, motivating the application of source apportionment analysis to the N-containing fragments only.

3.3. PMF on organic nitrogen (ON)

3.3.1. Selection and overview of the PMF ON solution

A 5-factor solution was chosen as the best representation of the PMF ON dataset. The retrieved factors were defined as: Oxygenated secondary OA (OOA_{ON}), amine-related OA ($AMOA_{ON}$), hydrocarbon-like OA (HOA_{ON}), industry OA (IOA_{ON}), and local primary OA (POA_{ON}).

The criterion used to determine the optimal number of factors is the examination of Q/Q_{exp} variations for an increasing number of solutions to evaluate the fraction of explained variation in the dataset. For the PMF ON solutions, the Q/Q_{exp} value decreases sharply from 3 to 1.7 as the number of factors increases from four to five, then becomes relatively flat as the number of factors increases to eight (Fig. S3). If the number of factors is decreased to four, a mixed OOA_{ON}/IOA_{ON} factor is retrieved, and a significant signature of IOA_{ON} is included in the OOA_{ON} factor (Fig. S4, S5, S6). Increasing the number of factors to six leads to non-interpretable splitting

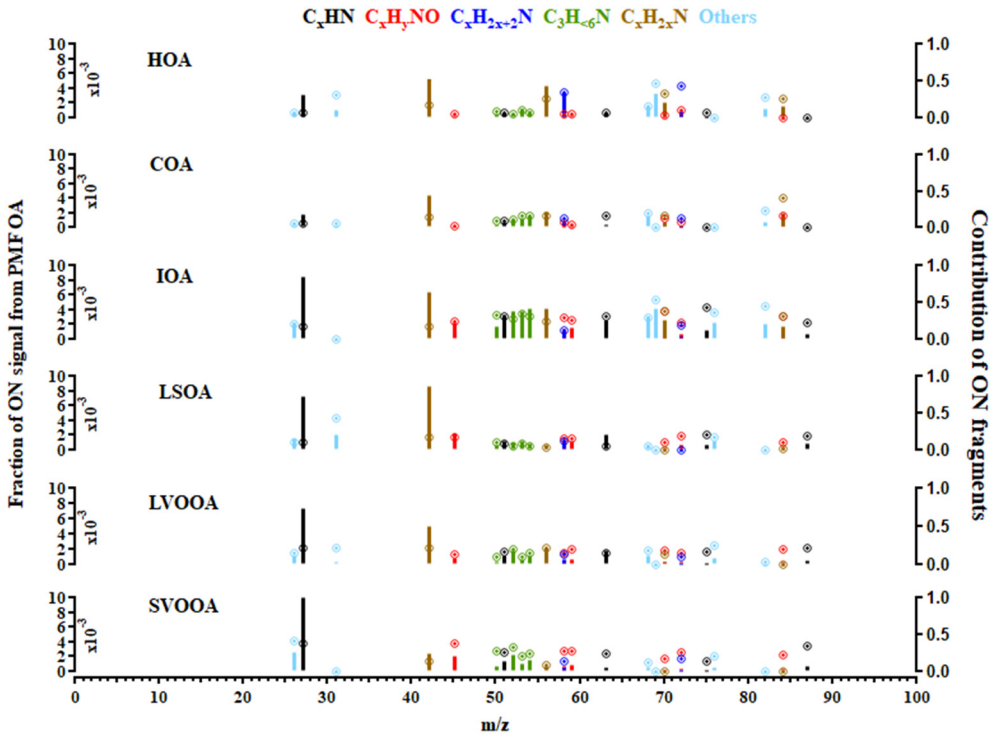

Fig. 2. ON apportionment in the original PMF of organic aerosol (PMF OA). The left axis for each factor profile presents the relative composition of each given ON ions and the right axis the relative contribution of each factor to the ion.

of the amine-related factor, which has a mass spectrum similar to the OOA_{ON} factor, rather than a "new" split factor.

Fig. 3 compares the absolute residual spectrum of ON ions derived from PMF ON analysis to the one of the PMF OA results. The PMF ON residuals are distributed around 0.005 μg m^{-3} with a maximum value of 0.007 μg m^{-3}. The scatter plot shows that the PMF ON residuals are generally lower than for the PMF OA. The PMF OA residuals show much larger values for some ions: C_2H_4N, $C_5H_{10}N$, and C_3H_6N (all belonging to the $C_xH_{2x}N$ family), as well as C_4H_7N, C_3H_8N, and CHN. Overall, the distinct mass spectral/relative contribution features in the PMF ON result and the distinctly lower residuals illustrate the improvement in comparison to PMF OA to identify the sources of ON species.

3.3.2. PMF ON factor descriptions

An overview of the factor time series, profiles, diurnal patterns and fractions of ON families is presented in Figs. 4 and 5. Each factor is described separately in further detail in the following sections. Fig. 6 shows the stacked time series of the concentrations of the factor contributions to each ON family and the corresponding pie charts.

3.3.2.1. Oxygenated OA (OOA_{ON}). The time series of the OOA_{ON} factor agrees well with the time variation of SOA_{OA}, i.e., the sum of $SVOOA_{OA}$, and $LVOOA_{OA}$ (r^2 = 0.67). In terms of the diurnal trend, the OOA_{ON} concentration, as shown in Fig. 5, displays no obvious difference between day and night.

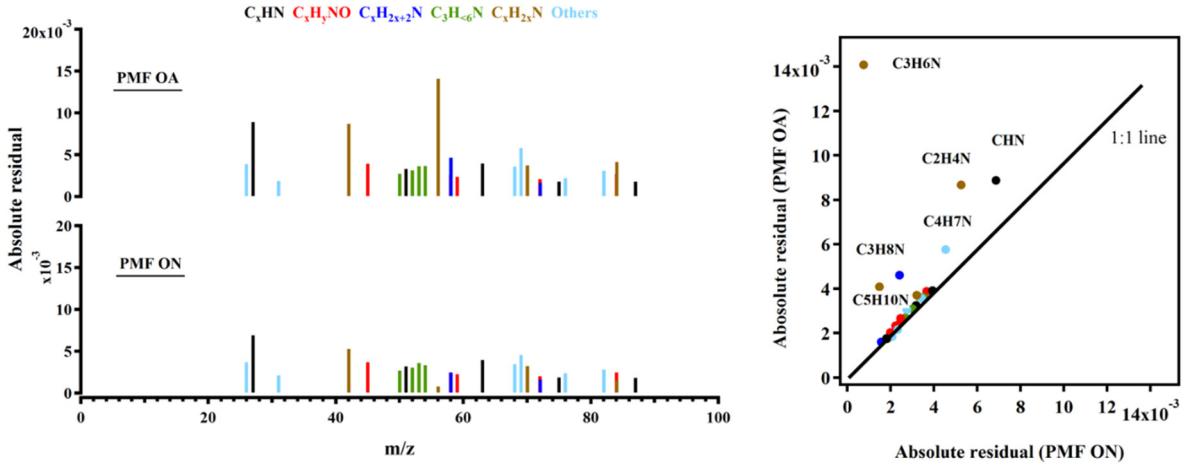

Fig. 3. Comparison of absolute residuals (ug m^{-3}) of ON ions between PMF OA and PMF ON, colored by the different ion families (left). Scatter plot of absolute residuals (ug m^{-3}) in the accepted solutions of PMF_ON and PMF_OA results (right).

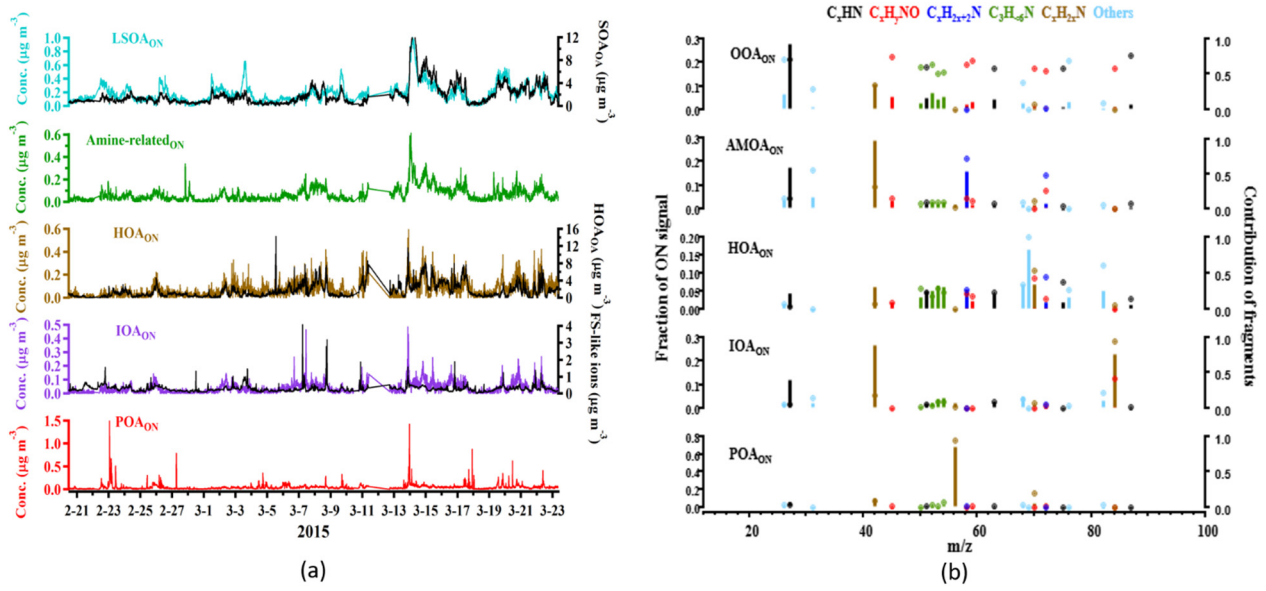

Fig. 4. Overview of the results from the organic nitrogen positive matrix factorization (PMF ON) analysis including time series (a) and factor profiles (b). In (b), the left axis for each factor profile presents the relative composition of each factor and the right axis the relative contribution of each factor to the given ON ions.

The profile of the OOA_{ON} factor shows the major ions are CHN^+ (m/z = 27) and $C_2H_4N^+$ (m/z = 42). Approximately 71% of the CHN^+ ion is apportioned to the OOA_{ON} factor (Fig. 4b), while $C_2H_4N^+$ is also apportioned in appreciable amounts to other factors. The OOA_{ON} mass spectrum is also dominated by the C_xHN^+ family including the ions CHN^+, C_3HN^+, C_4HN^+, C_5HN^+, and C_6HN^+, as well as the C_xH_yON and $C_3H_{<6}N$ families (Fig. 4 and Fig. 6a, b). These three families are apportioned to the factor with 68%, 66%, and 59%, respectively, as shown in Fig. 6. The C_xH_yON family includes six ions: CH_3NO (m/z = 45.02), C_2H_4NO (m/z = 58.03), C_2H_5NO (m/z = 59.04), C_3H_4NO (m/z = 70.03), C_3H_6NO (m/z = 72.05), and C_4H_6NO (m/z = 84.05), and their fractional contributions to OOA_{ON} are 73%, 64%, 69%, 58%, 54%, and 59%, respectively. This shows the main role of the C_xH_yON family in this factor and the presence of amides or amino acids. In contrast, the $C_3H_{<6}N$ family is distributed to other factors.

3.3.2.2. Amine-related OA ($AMOA_{ON}$). Amine fragments usually have small signals in HR-AMS datasets, and are typically difficult to identify because they are embedded in larger signals of adjacent peaks in the high resolution mass spectrum. The PMF ON analysis presents the amine-related OA factor as a separated ON contributor.

The time series of $AMOA_{ON}$ and nitrate (NO_3), which is often formed more locally and semi-volatile, are correlated, with r^2 = 0.45. The diurnal trends of NO_3_org and $AMOA_{ON}$ agree well with each other except for the period from 0:00 to 10:00 (Fig. 5), which indicates our $AMOA_{ON}$ factor might be closely related to anthropogenic emissions (Ng et al., 2008). During the day, this factor is inversely related to ozone, and decreases to its lowest value with the increasing radiation at noon.

Except for the two ions mentioned above (CHN^+ and $C_2H_4N^+$), the mass spectrum of the factor is mainly dominated by the $C_xH_{2x+2}N$ family ($C_3H_8N^+$, $C_4H_{10}N^+$, Fig. 6). Fig. 6c shows the fractional contributions of the $C_xH_{2x+2}N$ family to each factor, it's obvious that the ions in the $C_xH_{2x+2}N$ family mostly contribute to the $AMOA_{ON}$ factor (68%). Ion peaks corresponding to the $C_xH_{2x+2}N$ family are indicative of aliphatic amines which have been identified in ambient aerosols collected from a variety of sites (Pratt et al., 2009;Ge et al., 2011). The mass spectrum is unique in the PMF ON result, with specific amine fragments, compared to the PMF OA analysis (Fig. 2).

3.3.2.3. Hydrocarbon-like OA (HOA_{ON}). The factor is verified by the overall similar diurnal profiles of HOA_{ON} and HOA_{OA}, as shown in Fig. 5c, where both time series peak at times corresponding to rush hour traffic. The morning peak of HOA_{ON} is observed between 8:00 and 10:00, with the same variation as the HOA_{OA} factor. The evening peak of HOA_{ON} is relatively broad (18:00–22:00) with a maximum at 18:00–19:00, which is consistent with the rush hour from the HOA_{OA} factor which however has an additional peak at 21:00.

The mass spectrum is mainly dominated by $C_4H_7N^+$ (m/z = 69.06), only contributing to the HOA_{ON} factor (100%). This ion can thus be regarded to be a tracer of the HOA_{ON} factor. The factor also has higher contributions from $C_4H_8N^+$ (m/z = 70.07, Fig. 4) and $C_4H_6N^+$ (m/z = 68.05). In addition, the families $C_xH_{2x+2}N$ (apportioned to 29% in this factor), $C_3H_{<6}N$ (apportioned to 24%, excluding C_3HN, which belongs to the C_xHN family) and $C_xH_{2x}N$ (24%, including the ions $C_2H_4N^+$, $C_3H_6N^+$, $C_4H_8N^+$, $C_5H_{10}N^+$) are also apportioned to the HOA_{ON} factor. The $C_xH_{2x+2}N$ family mentioned above only contributes to $AMOA_{ON}$ and HOA_{ON} (Ye et al., 2017; Ge et al., 2011).

3.3.2.4. Industry OA (IOA_{ON}). We attribute this factor to Industry OA due to the high correlation of its diurnal variation with the ones of fullerene ions and *r*BC (Fig. 5), as reported by Wang et al., 2016. The mass spectrum of the factor contains enhanced peaks at m/z = 42 ($C_2H_4N^+$) and m/z = 84 ($C_5H_{10}N^+$). The relative contribution of $C_5H_{10}N^+$ is as high as 95% (Fig. 4b).

Industry emission was recognized as an important source of aerosols at the sampling site by the previous studies (Wu et al., 2018). A large number of petrochemical plants are situated northeast of the site (see Wang et al. (2016) for a distribution of industrial plants around this site), and during the campaign, winds mostly blew from this direction. The average diurnal pattern of fullerene ions displays a bimodal distribution with one prominent peak at 9:00 local time and another peak at 21:00 but overall remains elevated during daytime (Fig. 5). Indeed, the fullerene ions correlate poorly with all secondary species, including nitrate (r^2 = 0.08), sulfate (r^2 = 0.15), chloride (r^2 = 0.07), SVOOA (r^2 = 0.07), LVOOA (r^2 = 0.06), and LSOA (r^2 = 0.07), and even primary species such as COA (r^2 = 0.06) and HOA (r^2 = 0.12) but correlate much better with IOA (r^2 = 0.45). Furthermore, we applied a multilinear decomposition algorithm to estimate the contributions from traffic and industry to these fullerene ions: tsFullerenes = a × tsHOA + b × tsIOA, where tsFullerenes, tsHOA, and

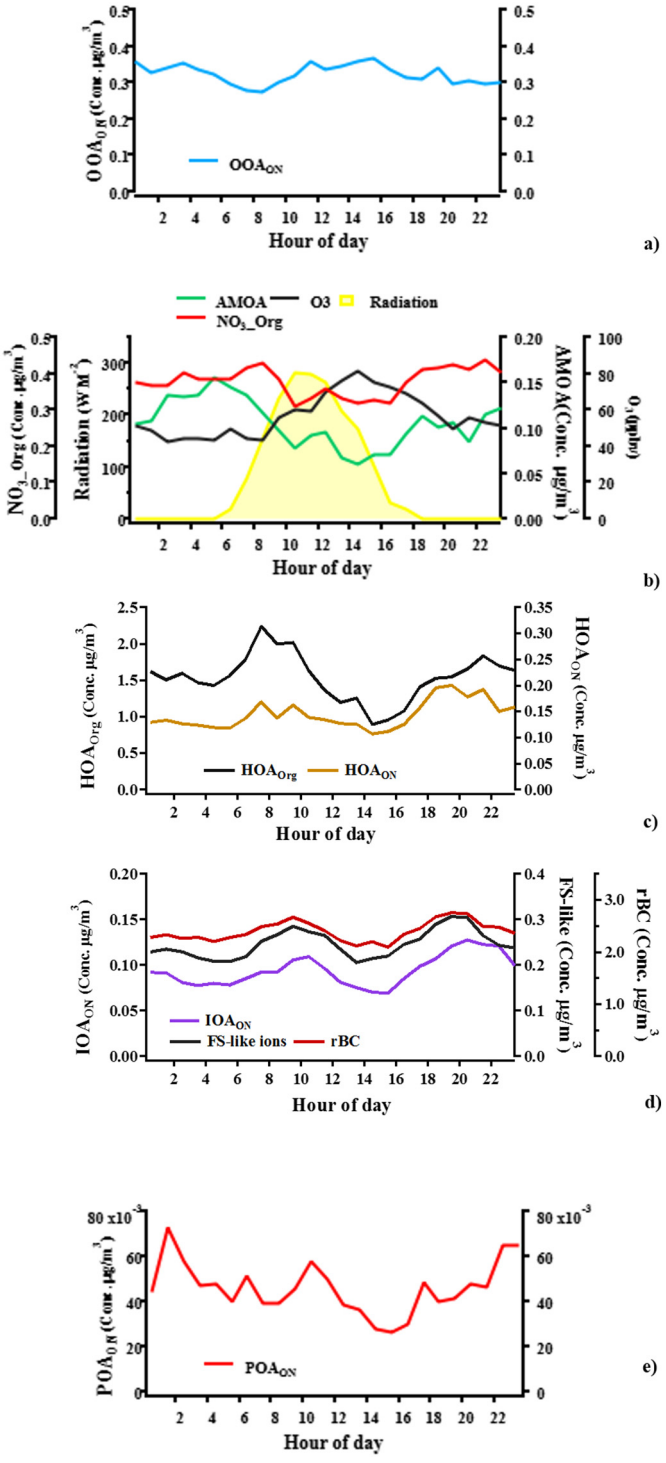

Fig. 5. Diurnal variations of the HOA_{ON}, $AMOA_{ON}$, OOA_{ON}, IOA_{ON}, and POA_{ON} factors and various tracer species.

tsIOA are the time series of fullerene ions, HOA, and IOA, respectively, and *a* and *b* are the fitting parameters. The reconstructed fullerene ion concentrations correlate reasonably well with the measured values [$r^2 = 0.52$ and a slope of 0.92] validating the effectiveness of this analysis, which yields a relative contribution of 70% from industry and 30% from traffic for the observed fullerene ions.

3.3.2.5. Local primary OA (POA_{ON}). The mass profile of the POA_{ON} factor is specific, in having the dominating ion $C_3H_6N^+$ (m/z = 56, 68%), with 99% of this ion contributing to this factor (Fig. 4b). The factor is near-zero except for a few periods: 22–23 February, 26 February, 13–15 March, and 17–21 March, in which periods all the factors have enhanced values. The diurnal trend is also unique without any tracer for comparison, as shown in Fig. 5. Here, we identify this factor as events-driven factor from local primary emission due to no obvious variation of the time series.

3.4. Comparison of PMF OA and PMF ON

The source separation and contribution of organic nitrogen ions/families between PMF ON and PMF OA results are compared in this section. Fig. 7 presents the stacked time series of the concentrations of these families in the PMF OA results representing the contributions of each factor to the total concentrations and the corresponding pie charts, analogous to the PMF ON presentation in Fig. 6.

As discussed in Section 3.3.2 and Section 3.3.4, the ON profiles in the POA_{OA} factors (HOA_{OA}, COA_{OA}, IOA_{OA}) derived from PMF OA source apportionment have no distinct features. In contrast, distinct mass spectral features in the PMF ON result are obvious, e.g. $C_4H_7N^+$ is almost only contributing to HOA_{ON}, $C_3H_6N^+$ is dominating in the POA_{ON} factor, and $C_5H_{10}N^+$ is to up to 95% apportioned to the IOA_{ON} factor. As discussed in the residual comparison (Fig. 3), most of the $C_xH_{2x+2}N$ ions have higher residuals which were not explained in the PMF OA analysis (Fig. S7), but they are identified in the PMF ON analysis as an amine-related factor. The contribution of the $C_3H_{<6}N$ family indicates high contributions to the IOA_{OA} and HOA_{ON} factors.

Fig. 7 compares the stacked time series of the PMF ON factors (Fig. 7a), the stacked time series of the sum of organic nitrogen ions in each of the PMF OA factors (Fig. 7b), and the stacked time series of the PMF OA factors (Fig. 7c). Also shown are pie charts of the mean PMF ON factor contributions over the entire measurement period, the mean ON contributions in each PMF OA factor, and the mean PMF OA factor contributions.

The HOA_{ON} (11%) and HOA_{OA} (14%, only ON content) are associated well with each other, the IOA_{ON} (18%) is lower than the IOA_{OA} (27%), and the sum (48%) of $LSOA_{OA}$ (14%), $LVOOA_{OA}$ (14%), and $SVOOA_{OA}$ (20%) correlates with OOA_{ON} (46%). As shown in Fig. S2, the good correlation between ON and OA might be driven by the time series of SOA_{OA} and OOA_{ON}. The POA_{ON} is a specific factor in the PMF ON analysis, more related to local emissions, which is probably mixed to the IOA_{OA}. The organic nitrogen compounds from COA are likely amines from meat or overcooked food, e.g. charbroiling, since reactions of fatty acids with ammonia at high temperature can yield amides (Lejay et al., 2019). Although it is hard to identify the COA factor in the PMF ON analysis, the amine-related factor (16%) is separated in PMF ON which indicates the amine-related emission sources particularly. Above all, the distribution of the PMF ON analysis shows clearly that there are significant contributions of organic nitrogen from SOA and HOA, while the organic nitrogen ions are distributed to each factor combining other OA ions in PMF OA analysis, hindering the understanding of organic nitrogen sources.

4. Conclusions

An Aerodyne SP-AMS was deployed in a suburban site of Nanjing, China from February 20 to March 23, 2015. In this study, we demonstrated the capability of the SP-AMS in quantification and characterization of organic nitrogen in atmospheric aerosols. Positive matrix factorization (PMF) was applied to the ON data to quantify the sources of ON in submicron aerosols. Five factors are retrieved as: Oxygenated OA (OOA_{ON}, well correlated with the SOA_{OA} factor and dominated by the CHN^+ ion and the C_xH_yON family), amine-related OA ($AMOA_{ON}$, correlating with nitrate with mostly contributions from the $C_xH_{2x+2}N$ family), hydrocarbon-like OA (HOA_{ON}, with concentration peaks at times corresponding to rush hour traffic and mainly dominated by the $C_4H_7N^+$ ion, which only contributed to this HOA_{ON} factor), industry OA (IOA_{ON}, with high correlation with fullerene ions and contributions from $C_2H_4N^+$ and $C_5H_{10}N^+$), and local primary OA (POA_{ON}, with a unique time series and dominated by the $C_3H_6N^+$ ion (m/z = 56, 68%), with 95%contribution to this factor).

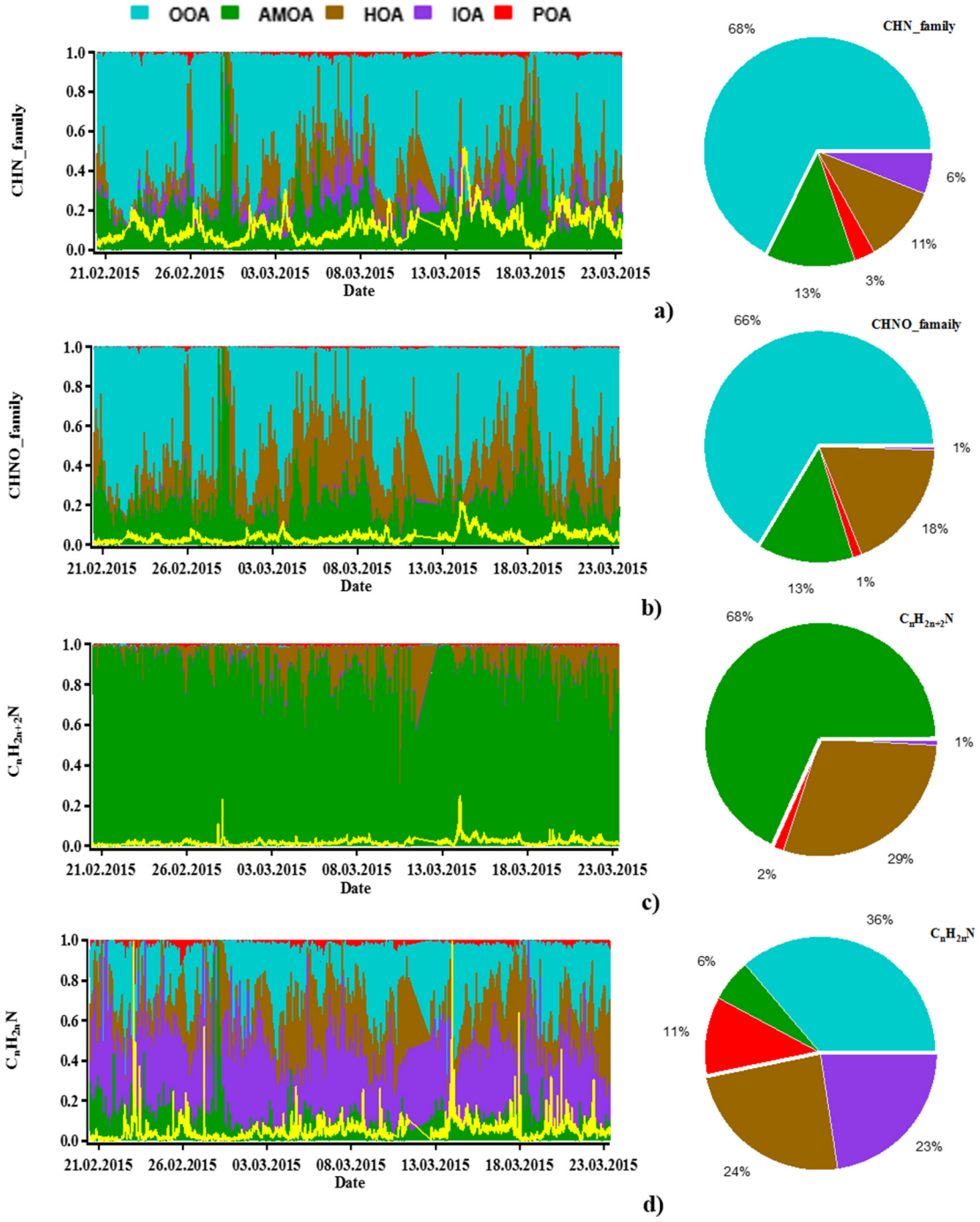

Fig. 6. Time series and fractional factor contributions as derived from the PMF ON solution (left) and corresponding pie charts (right) of the selected families C_xHN (a), C_xH_yNO (b), $C_xH_{2x+2}N$ (c), and $C_xH_{2x}N$ (d).

In the original PMF OA analysis, no specific ON mass spectral signature and/or striking differences of relative contributions of these ON ions to each factor were identified since almost all families and all ions appeared in each factor. The distinctly lower residual without much variation derived from the PMF ON results and distinct mass spectral/relative contribution features in the PMF ON result provide a new insight of our methodology to identify the sources of ON species.

CRediT authorship contribution statement

Lu Qi: Methodology, Software, Validation, Formal analysis, Investigation, Writing – original draft, Writing – review & editing, Visualization. **Carlo Bozzetti:** Methodology, Investigation, Software, Writing – review & editing. **Joel C. Corbin:** Methodology, Software, Formal analysis, Writing – review & editing. **Kaspar R. Daellenbach:** Investigation, Writing – review & editing. **Imad El Haddad:** Formal analysis, Investigation, Writing – review & editing. **Qi Zhang:** Resources, Supervision. **Junfeng Wang:** Methodology, Resources. **Urs Baltensperger:** Writing – review & editing, Supervision. **André S.H. Prévôt:** Writing – review & editing, Supervision, Project administration, Funding acquisition. **Mindong Chen:** Writing – review & editing, Supervision. **Xinlei Ge:** Methodology, Resources, Writing – review & editing, Supervision, Project administration, Funding acquisition. **Jay G. Slowik:** Formal analysis, Investigation, Writing – review & editing, Supervision.

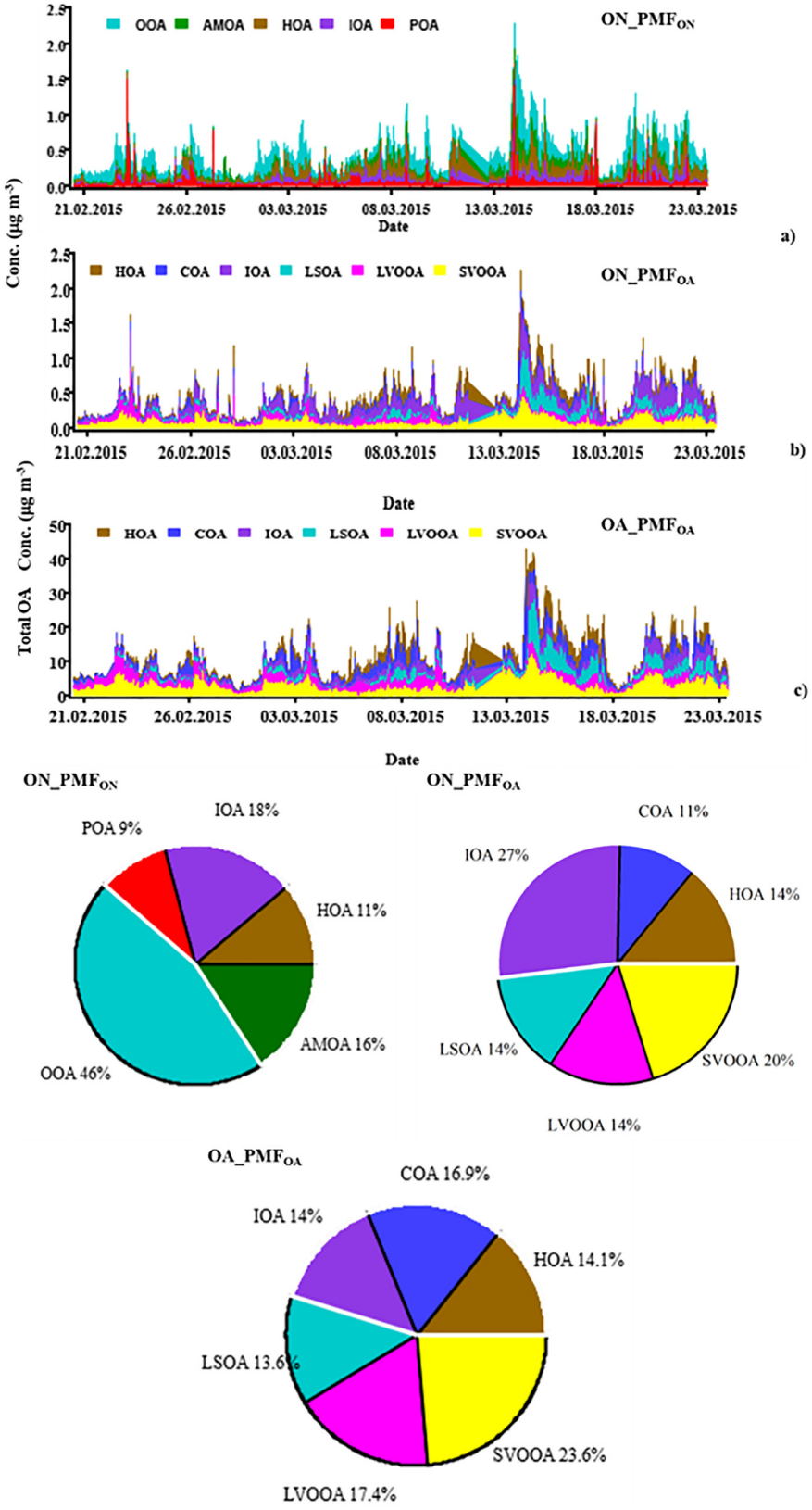

Fig. 7. Comparison between organic nitrogen (ON) factors and factors from the original PMF: time series of the concentrations of each organic nitrogen PMF ON factors (a) and organic nitrogen contribution for each original PMF OA factor (b), time series of each factor from PMF OA (c). Pie charts of the mean PMF ON factor contributions over the entire measurement period, the mean ON contributions in each PMF OA factor, and the mean PMF OA factor contributions.

Declaration of competing interest

The authors declare that they have no conflict of interests that could have appeared to influence the work reported in this paper.

Acknowledgements

This study was financially supported by China National Science Foundation projects (21976093, 21777073). We acknowledge the support by SNSF project HAZECHINA (IZLCZ2_169986).

Appendix A. Supplementary data

Supplementary data to this article can be found online at https://doi.org/10.1016/j.scitotenv.2021.151800.

References

Aiken, A.C., DeCarlo, P.F., Jimenez, J.L., 2007. Elemental analysis of organic species with electron ionization high-resolution mass spectrometry. Anal. Chem. 79, 8350–8358. https://doi.org/10.1021/Ac071150w.

Aiken, A.C., Decarlo, P.F., Kroll, J.H., Worsnop, D.R., Huffman, J.A., Docherty, K.S., Ulbrich, I.M., Mohr, C., Kimmel, J.R., Sueper, D., Sun, Y., Zhang, Q., Trimborn, A., Northway, M., Ziemann, P.J., Canagaratna, M.R., Onasch, T.B., Alfarra, M.R., Prevot, A.S.H., Dommen, J., Duplissy, J., Metzger, A., Baltensperger, U., Jimenez, J.L., 2008. O/C and OM/OC ratios of primary, secondary, and ambient organic aerosols with high-resolution time-of-flight aerosol mass spectrometry. Environ. Sci. Technol. 42, 4478–4485. https://doi.org/10.1021/Es703009q.

Aiken, A.C., Salcedo, D., Cubison, M.J., Huffman, J.A., DeCarlo, P.F., Ulbrich, I.M., Docherty, K.S., Sueper, D., Kimmel, J.R., Worsnop, D.R., Trimborn, A., Northway, M., Stone, E.A., Schauer, J.J., Volkamer, R.M., Fortner, E., de Foy, B., Wang, J., Laskin, A., Shutthanandan, V., Zheng, J., Zhang, R., Gaffney, J., Marley, N.A., Paredes-Miranda, G., Arnott, W.P., Molina, L.T., Sosa, G., Jimenez, J.L., 2009. Mexico City aerosol analysis during MILAGRO using high resolution aerosol mass spectrometry at the urban supersite (T0) - part 1: fine particle composition and organic source apportionment. Atmos. Chem. Phys. 9, 6633–6653. https://doi.org/10.5194/acp-9-6633-2009.

Angelino, S., Suess, D.T., Prather, K.A., 2001. Formation of aerosol particles from reactions of secondary and tertiary alkylamines: characterization by aerosol time-of-flight mass spectrometry. Environ. Sci. Technol. 35, 3130–3138. https://doi.org/10.1021/es0015444.

Bruns, E.A., Perraud, V., Zelenyuk, A., Ezell, M.J., Johnson, S.N., Yu, Y., Imre, D., Finlayson-Pitts, B.J., Alexander, M.L., 2010. Comparison of FTIR and particle mass spectrometry for the measurement of particulate organic nitrates. Environ. Sci. Technol. 44, 1056–1061. https://doi.org/10.1021/es9029864.

Canagaratna, M.R., Jayne, J.T., Jimenez, J.L., Allan, J.D., Alfarra, M.R., Zhang, Q., Onasch, T.B., Drewnick, F., Coe, H., Middlebrook, A., Delia, A., Williams, L.R., Trimborn, A.M., Northway, M.J., DeCarlo, P.F., Kolb, C.E., Davidovits, P., Worsnop, D.R., 2007. Chemical and microphysical characterization of ambient aerosols with the aerodyne aerosol mass spectrometer. Mass Spectrom. Rev. 26, 185–222. https://doi.org/10.1002/Mas.20115.

Canagaratna, M.R., Jimenez, J.L., Kroll, J.H., Chen, Q., Kessler, S.H., Massoli, p., Hildebrandt Ruiz, L., Fortner, E., Williams, L.R., Wilson, K.R., Surratt, J.D., Donahue, N.M., Jayne, J.T., Worsnop, D.R., 2015. Elemental ratio measurements of organic compounds using aerosol mass spectrometry: characterization, improved calibration, and implications. Atmos. Chem. Phys. 15, 253–272. https://doi.org/10.5194/acp-15-253-2015 In this issue.

Canonaco, F., Crippa, M., Slowik, J.G., Baltensperger, U., Prévôt, A.S.H., 2013. SoFi, an IGOR-based interface for the efficient use of the generalized multilinear engine (ME-2) for the source apportionment: ME-2 application to aerosol mass spectrometer data. Atmos. Meas. Tech. 6, 3649–3661. https://doi.org/10.5194/amt-6-3649-2013.

Cape, J.N., Cornell, S.E., Jickells, T.D., Nemitz, E., 2011. Organic nitrogen in the atmosphere — where does it come from? A review of sources and methods. Atmos. Res. 102, 30–48. https://doi.org/10.1016/j.atmosres.2011.07.009.

Chan, M.N., Choi, M.Y., Ng, N.L., Chan, C.K., 2005. Hygroscopicity of water-soluble organic compounds in atmospheric aerosols: amino acids and biomass burning derived organic species. Environ. Sci. Technol. 39, 1555–1562. https://doi.org/10.1021/Es049584l.

Chen, Y., Ge, X., Chen, H., Xie, X., Chen, Y., Wang, J., Ye, Z., Bao, M., Zhang, Y., Chen, M., 2018. Seasonal light absorption properties of water-soluble brown carbon in atmospheric fine particles in Nanjing, China. Atmos. Environ. https://doi.org/10.1016/j.atmosenv.2018.06.002.

Chen, Y., Chen, Y., Xie, X., Ye, Z., Li, Q., Ge, X., Chen, M., 2019. Chemical characteristics of PM2. 5 and water-soluble organic nitrogen in Yangzhou, China. Atmosphere 10 (4), 178. https://doi.org/10.3390/atmos10040178.

Chen, Y., Xie, X., Shi, Z., Li, Y., Gai, X., Wang, J., Li, H., Wu, Y., Zhao, X., Chen, M., Ge, X., 2020. Brown carbon in atmospheric fine particles in Yangzhou, China: Light absorption properties and source apportionment. Atmos. Res. 244, 105028. https://doi.org/10.1016/j.atmosres.2020.105028.

Clegg, S.L., Qiu, C., Zhang, R., 2013. The deliquescence behaviour, solubilities, and densities of aqueous solutions of five methyl- and ethyl-aminium sulphate salts. Atmos. Environ. 73, 145–158. https://doi.org/10.1016/j.atmosenv.2013.02.036.

Corbin, J.C., Sierau, B., Gysel, M., Laborde, M., Keller, A., Kim, J., Petzold, A., Onasch, T.B., Lohmann, U., Mensah, A.A., 2014. Mass spectrometry of refractory black carbon particles from six sources: carbon-cluster and oxygenated ions. Atmos. Chem. Phys. 14, 2591–2603. https://doi.org/10.5194/acp-14-2591-2014.

Corbin, J.C., Othman, A., Haskins, D.J., Allan, D.J., Sierau, B., Worsnop, R.D., Lohmann, U., Mensah, A.A., 2015. Peak fitting and integration uncertainties for the aerodyne aerosol mass spectrometer. Atmos. Meas. Tech. 8 (4), 3471–3523. https://doi.org/10.5194/amtd-8-3471-2015.

Cornell, S., 2011. Atmospheric nitrogen deposition: revisiting the question of the importance of the organic component. Environ. Pollut. 159, 2214–2222. https://doi.org/10.1016/j.envpol.2010.11.014.

Cornell, S., Randell, A., Jickells, T., 1995. Atmospheric inputs of dissolved organic nitrogen to the oceans. Nature 376, 243–246. https://doi.org/10.1038/376243a0.

Cornell, S., Jickells, T.D., Cape, J.N., Rowland, A.P., Duce, R.A., 2003. Organic nitrogen deposition on land and coastal environments: a review of methods and data. Atmos. Environ. 37, 2173–2191. https://doi.org/10.1016/S1352-2310(03)00133-X.

Davison, A.C., Hinkley, D.V., 1997. Bootstrap Methods and Their Application. Cambridge University Press, Cambridge, New York, NY, USA.

DeCarlo, P.F., Kimmel, J.R., Trimborn, A., Northway, M.J., Jayne, J.T., Aiken, A.C., Gonin, M., Fuhrer, K., Horvath, T., Docherty, K.S., Worsnop, D.R., Jimenez, J.L., 2006. Field-deployable, high-resolution, time-of-flight aerosol mass spectrometer. Anal. Chem. 78, 8281–8289. https://doi.org/10.1021/Ac061249n.

Duan, F., Liu, X., He, K., Dong, S., 2009. Measurements and characteristics of nitrogen-containing compounds in atmospheric particulate matter in Beijing, China. Bull. Environ. Contam. Toxicol. 82 (3), 332–337. https://doi.org/10.1007/s00128-008-9560-0.

Farmer, D.K., Matsunaga, A., Docherty, K.S., Surratt, J.D., Seinfeld, J.H., Ziemann, P.J., Jimenez, J.L., 2010. Response of an aerosol mass spectrometer to organonitrates and organosulfates and implications for atmospheric chemistry. Proc. Natl. Acad. Sci. U. S. A. 107, 6670–6675. https://doi.org/10.1073/pnas.0912340107.

Fry, J.L., Kiendler-Scharr, A., Rollins, A.W., Wooldridge, P.J., Brown, S.S., Fuchs, H., Dubé, W., Mensah, A., dal Maso, M., Tillmann, R., Dorn, H.P., Brauers, T., Cohen, R.C., 2009. Organic nitrate and secondary organic aerosol yield from NO_3 oxidation of β-pinene evaluated using a gas-phase kinetics/aerosol partitioning model. Atmos. Chem. Phys. 9, 1431–1449. https://doi.org/10.5194/acp-9-1431-2009.

Fry, J.L., Draper, D.C., Zarzana, K.J., Campuzano-Jost, P., Day, D.A., Jimenez, J.L., Brown, S.S., Cohen, R.C., Kaser, L., Hansel, A., Cappellin, L., Karl, T., Hodzic Roux, A., Turnipseed, A., Cantrell, C., Lefer, B.L., Grossberg, N., 2013. Observations of gas- and aerosol-phase organic nitrates at BEACHON-RoMBAS 2011. Atmos. Chem. Phys. 13, 8585–8605. https://doi.org/10.5194/acp-13-8585-2013.

Ge, X.L., Wexler, A.S., Clegg, S.L., 2011. Atmospheric amines - Part I. A review. Atmos. Environ. 45, 524–546. https://doi.org/10.1016/j.atmosenv.2010.10.012.

Ho, K.F., Ho, S.S.H., Huang, R.-J., Liu, S.X., Cao, J.-J., Zhang, T., Chuang, H.-C., Chan, C.S., Hu, D., Tian, L., 2015. Characteristics of water-soluble organic nitrogen in fine particulate matter in the continental area of China. Atmos. Environ. 106, 252–261. https://doi.org/10.1016/j.atmosenv.2015.02.010.

Hu, D., Li, C., Chen, H., Chen, J., Ye, X., Li, L., Yang, X., Wang, X., Mellouki, A., Hu, Z., 2014. Hygroscopicity and optical properties of alkylaminium sulfates. J. Environ. Sci. 26, 37–43. https://doi.org/10.1016/S1001-0742(13)60378-2.

Huang, Chen, H., Wang, L., Yang, X., Chen, J.M., YLH, 2012. Single particle analysis of amines in ambient aerosol in Shanghai. Environmental Chemistry 9, 202–210. https://doi.org/10.1071/en11145.

Jayne, J.T., Leard, D.C., Zhang, X., Davidovits, P., Smith, K.A., Kolb, C.E., Worsnop, D.R., 2000. Development of an aerosol mass spectrometer for size and composition analysis of submicron particles. Aerosol Sci. Technol. 33, 49–70. https://doi.org/10.1016/S0021-8502(98)00158-X.

Jickells, T., Baker, A.R., Cape, J.N., Cornell, S.E., Nemitz, E., 2013. The cycling of organic nitrogen through the atmosphere. Philos. Trans. R. Soc., B 368. https://doi.org/10.1098/rstb.2013.0115.

Junninen, H., Ehn, M., Petäjä, T., Luosujärvi, L., Kotiaho, T., Kostiainen, R., Rohner, U., Gonin, M., Fuhrer, K., Kulmala, M., Worsnop, D.R., 2010. A high-resolution mass spectrometer to measure atmospheric ion composition. Atmos. Meas. Tech. 3, 1039–1053. https://doi.org/10.5194/amt-3-1039-2010.

Kiendler-Scharr, A., Mensah, A.A., Friese, E., Topping, D., Nemitz, E., Prevot, A.S.H., Aijala, M., Allan, J., Canonaco, F., Canagaratna, M., Carbone, S., Crippa, M., Dall Osto, M., Day, D.A., De Carlo, P., Di Marco, C.F., Elbern, H., Eriksson, A., Freney, E., Hao, L., Herrmann, H., Hildebrandt, L., Hillamo, R., Jimenez, J.L., Laaksonen, A., McFiggans, G., Mohr, C., O'Dowd, C., Otjes, R., Ovadnevaite, J., Pandis, S.N., Poulain, L., Schlag, P., Sellegri, K., Swietlicki, E., Tiitta, P., Vermeulen, A., Wahner, A., Worsnop, D., Wu, H.C., 2016. Ubiquity of organic nitrates from nighttime chemistry in the European submicron aerosol. Geophys. Res. Lett. 43 (7735–7744), 2016. https://doi.org/10.1002/2016GL069239.

Lee, A.K.Y., Zhao, R., Li, R., Liggio, J., Li, S.-M., Abbatt, J.P.D., 2013. Formation of light absorbing organo-nitrogen species from evaporation of droplets containing glyoxal and ammonium sulfate. Environ. Sci. Technol. 47, 12819–12826. https://doi.org/10.1021/es402687w.

Lejay, M., Alexis, M.A., Quenea, K., Anquetil, C., Bon, F., 2019. The organic signature of an experimental meat-cooking fireplace: the identification of nitrogen compounds and their archaeological potential. Org. Geochem 138, 103923. https://doi.org/10.1016/j.orggeochem.2019.103923.

Lopez-Hilfiker, F.D., Mohr, C., Ehn, M., Rubach, F., Kleist, E., Wildt, J., Mentel, T.F., Lutz, A., Hallquist, M., Worsnop, D., Thornton, J.A., 2014. A novel method for online analysis of gas and particle composition: description and evaluation of a Filter Inlet for Gases and AEROsols (FIGAERO). Atmos. Meas. Tech. 7 (4), 983–1001. https://doi.org/10.5194/amt-7-983-2014 Apr 15.

Middlebrook, A.M., Bahreini, R., Jimenez, J.L., Canagaratna, M.R., 2012. Evaluation of composition-dependent collection efficiencies for the aerodyne aerosol mass spectrometer using field data. Aerosol Sci. Technol. 46, 258–271. https://doi.org/10.1080/02786826.2011.620041.

Mohr, C., Lopez-Hilfiker, F.D., Zotter, P., Prévôt, A.S., Xu, L., Ng, N.L., Herndon, S.C., Williams, L.R., Franklin, J.P., Zahniser, M.S., Worsnop, D.R., 2013. Contribution of nitrated phenols to wood burning brown carbon light absorption in Detling, United Kingdom during winter time. Environ. Sci. Technol. 47 (12), 6316–6324. https://doi.org/10.1021/es400683v.

Neff, J.C., Holland, E.A., Dentener, F.J., McDowell, W.H., Russell, K.M., 2002. The origin, composition and rates of organic nitrogen deposition: a missing piece of the nitrogen cycle? Biogeochemistry 57, 99–136. https://doi.org/10.1023/A:1015791622742.

Ng, N.L., Kwan, A.J., Surratt, J.D., Chan, A.W.H., Chhabra, P.S., Sorooshian, A., Pye, H.O.T., Crounse, J.D., Wennberg, P.O., Flagan, R.C., Seinfeld, J.H., 2008. Secondary organic aerosol (SOA) formation from reaction of isoprene with nitrate radicals (NO_3). Atmos. Chem. Phys. 8, 4117–4140. https://doi.org/10.5194/acp-8-4117-2008.

Nguyen, T.B., Lee, P.B., Updyke, K.M., Bones, D.L., Laskin, J., Laskin, A., Nizkorodov, S.A., 2012. Formation of nitrogen- and sulfur-containing light-absorbing compounds accelerated by evaporation of water from secondary organic aerosols. J. Geophys. Res.Atmos. 117. https://doi.org/10.1029/2011jd016944.

Onasch, T.B., Trimborn, A., Fortner, E.C., Jayne, J.T., Kok, G.L., Williams, L.R., Davidovits, P., Worsnop, D.R., 2012. Soot particle aerosol mass spectrometer: development, validation, and initial application. Aerosol Sci. Technol. 46, 804–817. https://doi.org/10.1080/02786826.2012.663948.

Onasch, T.B., Fortner, E.C., Trimborn, A.M., Lambe, A.T., Tiwari, A.J., Marr, L.C., Corbin, J.C., Mensah, A.A., Williams, L.R., Davidovits, P., Worsnop, D.R., 2015. Investigations of SP-AMS carbon ion distributions as a function of refractory black carbon particle type. Aerosol Sci. Technol. 49 (6), 409–422. https://doi.org/10.1080/02786826.2015.1039959.

Paatero, P., Tapper, U., 1994. Positive matrix factorization: a non-negative factor model with optimal utilization of error estimates of data values. Environmetrics 5, 111–126. https://doi.org/10.1002/env.3170050203.

Powelson, M.H., Espelien, B.M., Hawkins, L.N., Galloway, M.M., De Haan, D.O., 2013. Brown carbon formation by aqueous-phase carbonyl compound reactions with amines and ammonium sulfate. Environ. Sci. Technol. https://doi.org/10.1021/es4038325.

Pratt, K.A., Hatch, L.E., Prather, K.A., 2009. Seasonal volatility dependence of ambient particle phase amines. Environ. Sci. Technol. 43, 5276–5281. https://doi.org/10.1021/es803189n.

Qiu, C., Zhang, R., 2012. Physiochemical properties of alkylaminium sulfates: hygroscopicity, thermostability, and density. Environ. Sci. Technol. 46, 4474–4480. https://doi.org/10.1021/es3004377.

Ruiz-Jimenez, J., Hautala, S., Parshintsev, J., Laitinen, T., Hartonen, K., Petaja, T., Kulmala, M., Riekkola, M.L., 2012. Aliphatic and aromatic amines in atmospheric aerosol particles: comparison of three ionization techniques in liquid chromatography-mass spectrometry and method development. Talanta 97, 55–62. https://doi.org/10.1016/j.talanta.2012.03.062.

Samy, S., Hays, M.D., 2013. Quantitative LC–MS for water-soluble heterocyclic amines in fine aerosols (PM2.5) at Duke Forest, USA. Atmos. Environ. 72, 77–80. https://doi.org/10.1016/j.atmosenv.2013.02.032.

Samy, S., Robinson, J., Hays, M.D., 2011. An advanced LC-MS (Q-TOF) technique for the detection of amino acids in atmospheric aerosols. Anal. Bioanal. Chem. 401, 3103–3113. https://doi.org/10.1007/s00216-011-5238-2.

Samy, S., Robinson, J., Rumsey, I.C., Walker, J.T., Hays, M.D., 2013. Speciation and trends of organic nitrogen in southeastern U.S. fine particulate matter (PM2.5). https://doi.org/10.1029/2012JD017868 n/a-n/a.

Sauerwein, M., Clegg, S.L., Chan, C.K., 2015. Water activities and osmotic coefficients of aqueous solutions of five alkyl-aminium sulfates and their mixtures with H2SO4 at 25 °C. Aerosol Sci. Technol. 00–00. https://doi.org/10.1080/02786826.2015.1043045.

Saxena, P., Hildemann, L.M., 1996. Water-soluble organics in atmospheric particles: a critical review of the literature and application of thermodynamics to identify candidate compounds. J. Atmos. Chem. 24, 57–109. https://doi.org/10.1007/BF00053823.

Seitzinger, S.P., Sanders, R.W., 1999. Atmospheric inputs of dissolved organic nitrogen stimulate estuarine bacteria and phytoplankton. Limnol. Oceanogr. 44, 721–730. https://doi.org/10.4319/lo.1999.44.3.0721.

Smith, J.N., Barsanti, K.C., Friedli, H.R., Ehn, M., Kulmala, M., Collins, D.R., Scheckman, J.H., Williams, B.J., McMurry, P.H., 2010. Observations of aminium salts in atmospheric nanoparticles and possible climatic implications. Proc. Natl. Acad. Sci. 107, 6634–6639. https://doi.org/10.1073/pnas.0912127107.

Struckmeier, C., Drewnick, F., Fachinger, F., Gobbi, G.P., Borrmann, S., 2016. Atmospheric aerosols in Rome, Italy: sources, dynamics and spatial variations during two seasons. Atmos. Chem. Phys. 16, 15277–15299. https://doi.org/10.5194/acp-16-15277-2016.

Sun, Y.L., Zhang, Q., Schwab, J.J., Chen, W.N., Bae, M.S., Lin, Y.C., Hung, H.M., Demerjian, K.L., 2011a. A case study of aerosol processing and evolution in summer in New York City. Atmos. Chem. Phys. 11, 12737–12750. https://doi.org/10.5194/acp-11-12737-2011.

Sun, Y.L., Zhang, Q., Schwab, J.J., Demerjian, K.L., Chen, W.N., Bae, M.S., Hung, H.M., Hogrefe, O., Frank, B., Rattigan, O.V., Lin, Y.C., 2011b. Characterization of the sources and processes of organic and inorganic aerosols in New York city with a high-resolution time-of-flight aerosol mass apectrometer. Atmos. Chem. Phys. 11, 1581–1602. https://doi.org/10.5194/acp-11-1581-2011.

Wang, J., Onasch, T.B., Ge, X., Collier, S., Zhang, Q., Sun, Y., Yu, H., Chen, M., Prévôt, A.S.H., Worsnop, D.R., 2016. Observation of fullerene soot in eastern China. Environ. Sci. Technol. Lett. 3, 121–126. https://doi.org/10.1021/acs.estlett.6b00044.

Weathers, K.C., Lovett, G.M., Likens, G.E., Caraco, N.F.M., 2000. Cloudwater inputs of nitrogen to forest ecosystems in southern Chile: forms, fluxes, and sources. Ecosystems 3, 590–595.. http://www.jstor.org/stable/3658777.

Wu, Y., Ge, X., Wang, J., Shen, Y., Ye, Z., Ge, S., Wu, Y., Yu, H., Chen, M., 2018. Responses of secondary aerosols to relative humidity and photochemical activities in an industrialized environment during late winter. Atmos. Environ. 193, 66–78. https://doi.org/10.1016/j.atmosenv.2018.09.008.

Xu, L., Guo, H., Boyd, C.M., Klein, M., Bougiatioti, A., Cerully, K.M., Hite, J.R., Isaacman-VanWertz, G., Kreisberg, N.M., Knote, C., Olson, K., Koss, A., Hering, S.V., de Gouw, J., Baumann, K., Lee, S.-H., Nenes, A., Weber, R.J., Ng, N.L., 2015. Effects of anthropogenic emissions on aerosol formation from isoprene and monoterpenes in the southeastern United States. Proc. Natl. Acad. Sci. USA 112, E4506–E4507. https://doi.org/10.1073/pnas.1512277112.

Xu, W., Sun, Y., Wang, Q., Du, W., Zhao, J., Ge, X., Han, T., Zhang, Y., Zhou, W., Li, J., Fu, P., Wang, Z., Worsnop, D.R., 2017. Seasonal characterization of organic nitrogen in atmospheric aerosols using high resolution aerosol mass spectrometry in Beijing, China. ACS Earth Space Chem. 1, 673–682. https://doi.org/10.1021/acsearthspacechem.7b00106.

Ye, Z., Liu, J., Gu, A., Feng, F., Liu, Y., Bi, C., Xu, J., Li, L., Chen, H., Chen, Y., Dai, L., Zhou, Q., Ge, X., 2016. Chemical characterization of fine particulate matter in Changzhou, China, and source apportionment with offline aerosol mass spectrometry. Atmos. Chem. Phys. 17, 2573–2592. https://doi.org/10.5194/acp-17-2573-2017.

Ye, Z., Liu, J., Gu, A., Feng, F., Liu, Y., Bi, C., Xu, J., Li, L., Chen, H., Chen, Y., Dai, L., Zhou, Q., Ge, X., 2017. Chemical characterization of fine particular matter in Changzhou, China and source apportionment with offline aerosol mass spectrometry. Atmos. Chem. Phys. 17, 2573–2592. https://doi.org/10.5194/acp-17-2573-2017.

Yu, K., Zhu, Q., Du, K., Huang, X.-F., 2019. Characterization of nighttime formation of particulate organic nitrates based on high-resolution aerosol mass spectrometry in an urban atmosphere in China. Atmos. Chem. Phys. 19, 5235–5249. https://doi.org/10.5194/acp-19-5235-2019.

Zarzana, K.J., De Haan, D.O., Freedman, M.A., Hasenkopf, C.A., Tolbert, M.A., 2012. Optical properties of the products of alpha-dicarbonyl and amine reactions in simulated cloud droplets. Environ. Sci. Technol. 46, 4845–4851. https://doi.org/10.1021/es2040152.

Zhang, Q., Anastasio, C., 2001. Chemistry of fog waters in California's Central Valley - part 3: concentrations and speciation of organic and inorganic nitrogen. Atmos. Environ. 35, 5629–5643. https://doi.org/10.1016/S1352-2310(01)00337-5.

Zhang, Q., Anastasio, C., 2003. Free and combined amino compounds in atmospheric fine particles (PM2.5) and fog waters from Northern California. Atmos. Environ. 37, 2247–2258. https://doi.org/10.1016/s1352-2310(03)00127-4.

Zhang, Q., Anastasio, C., Jimemez-Cruz, M., 2002. Water-soluble organic nitrogen in atmospheric fine particles (PM2.5) from northern California. J. Geophys. Res. Atmos. 107. https://doi.org/10.1029/2001jd000870.